



室蘭工業大学

学術資源アーカイブ

Muroran Institute of Technology Academic Resources Archive



A Four-Legged Mobile Robot with Prismatic Joints on Spiral Footholds

メタデータ	言語: eng 出版者: 室蘭工業大学 公開日: 2016-03-25 キーワード (Ja): キーワード (En): Mobile robot, Legged robot, Wetland, Environmental survey, Robot motion 作成者: 花島, 直彦, 劉, 群坡, 梶原, 秀一 メールアドレス: 所属:
URL	http://hdl.handle.net/10258/00008608

A Four-Legged Mobile Robot with Prismatic Joints on Spiral Footholds

著者	HANAJIMA Naohiko, LIU Qunpo, KAJIWARA Hidekazu
journal or publication title	Memoirs of the Muroran Institute of Technology
volume	65
page range	23-29
year	2016-03-25
URL	http://hdl.handle.net/10258/00008608

A Four-Legged Mobile Robot with Prismatic Joints on Spiral Footholds

Naohiko HANAJIMA* Qunpo LIU** Hidekazu KAJIWARA***

(Received 26th October 2015, Accepted 2nd February 2016)

Abstract

This paper addresses a new design of a four-legged mobile robot with a double-spiral mobile architecture. The double-spiral mobile architecture has been proposed with the intention of use for environmental surveys in wetlands, where reed-like plants grow densely. It consists of two pairs of spirals and one mobile robot. Each pair of spirals plays the role of footholds for the mobile robot. By traveling at a higher place from the ground, the robot can avoid strong resistance force from the dense and hard-stemmed plants. In addition, the spirals intermediate between the robots and the muddy ground to avoid sinking. The proposed leg mechanism does not have any vertical movement. It contributes to energy saving in the robot. Also it provides the arbitrary motion of the body platform while the legs grip the spirals tightly. We derive the robot's kinematics and statics and show the validity of the design mathematically.

Keywords: Mobile robot, Legged robot, Wetland, Environmental survey, Robot motion

1 INTRODUCTION

The problem regarding the reduction of wetlands areas has come to occupy an important position in environmental conservation. In Kushiro Mire, which is the largest wetland in Japan, the distribution areas of alder forests or Sasa (veitchii) are increasing and a nature restoration project has been started. To investigate the mechanisms of its degradation trend, much effort is put into field surveys.

If we use a remote-sensing system, we can obtain spatially wide data, such as radar images or visible images from satellites. However, if we need more precise physical data, a field survey is mandatory. In field surveys, researchers must bring large quantities of tools into the field. Since entering into wetlands in vehicles is restricted, researchers find it difficult to

walk around huge areas in the muddy soil of the wetlands. Therefore, a technical support system for field survey in the wetlands is required.

Recently there are increasing developments in outdoor applications such as agriculture robots⁽¹⁾, automatic driving cars⁽²⁾ rescue robots⁽³⁾ and so on. However, in wetland applications, conventional locomotion mechanisms may cause serious problems. For example, wheel mechanisms may easily become stuck in the mud. Crawler mechanisms may tread on vegetation in the wetlands or turn over on hard-stemmed plants like Phragmites. Some special mechanisms using screws, which are called marsh screw amphibians, were developed and tested⁽⁴⁾ in the wetlands⁽⁵⁾. The size is about that of a passenger car, and very deep tracks like a ditch are left behind the screws that damage the surface of the earth severely. The other robots which have the same mechanism using screws were found in the literature⁽⁶⁾. New locomotion mechanisms suitable for the wetlands, which suppress damage to the vegetation and do not

* College of Design and Manufacturing Technology

** School of Electrical Engineering and Automation, Henan Polytechnic University

*** College of Information and Systems

sink in the mud, should be developed.

The double-spiral mobile architecture has been proposed with the intention of use for environmental surveys in the wetland where reed-like plants grow densely⁽⁷⁾. It consists of two pairs of spirals and one mobile robot. Each pair of spirals plays the role of footholds for the mobile robot. By traveling at a higher distance from the ground, the robot can avoid strong resistance force from the dense and hard-stemmed plants. In addition, since the spiral is supported by several contact points on the ground and intermediates between the robot and the muddy ground, the robot never touches the ground and barely sinks.

The mobile robot proposed in this paper has four legs for static walking on the spirals. A pair of spirals is aligned on a central axis and meshes with each other. Two pairs of the spirals are horizontally aligned on the ground side by side. In stance phase of the robot's gait, the mobile robot stands on the spirals so that two legs on one side of the robot are placed on one of the spirals on the same side. The other spirals, which do not support the robot, rotate and thread their way through dense, tall plants with hard stems. After that, the robot steps forward. In swing phase of the robot gait, the robot moves its legs to the rotated spirals.

The main features of the proposed robot in this paper are in the design of the mechanism of the legs. First of all, one mechanism on the end portion of each leg is in a gantry shape. Unlike a typical legged robot, this mechanism realizes the swing phase without any vertical motion. This contributes simple mechanisms and energy savings for the robot.

Second, each leg has two prismatic joints orthogonal to each other and one rotational joint for 3 DOF (degrees of freedom) motion in a plane. This provides the body platform with arbitrary planar motion in its own plane.

In the rest of this paper, we show the conceptual design of the robot. Next, we derive the kinematics of the robot. Then, we show the validity of the design mathematically.

2 MATERIALS AND METHODS

Figure 1 shows the conceptual image of the robot that we propose in this paper. As mentioned in the introductory part, it consists of two pairs of spirals and one mobile robot. In this section, we explain the requirements for the robot to walk on the spiral properly. Then we show how the proposed robot satisfies the requirements and its step motion to the next footing. Next, we define the coordinate systems for each link of the robot to prepare for a formulation of kinematics of the robot. Practical sizes of the robot are discussed from the point of view of the resistance received from the plants.

2.1 Requirements for walking on the spirals

In order to carry burdens on the robot securely, the robot needs to maintain its posture while walking. The robot walking on the spirals is required not to tumble over in gait, not to slip off the spirals, not to lose its footing, not to roll over together with a gripping spiral, and to move in the desired direction. However, it is not required to move rapidly. These five requirements contribute to realizing secure walking.

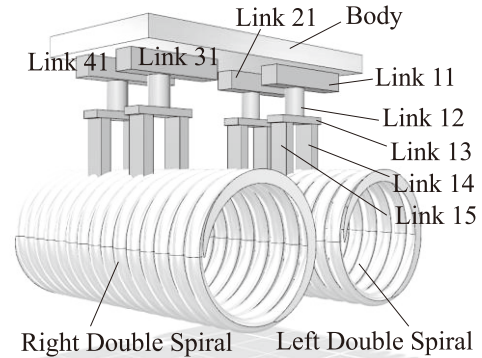


Figure 1 Conceptual design of the proposed robot

2.2 Four-legged locomotion and the gait

We adopt four-legged locomotion and a creep gait for our walking robot. Generally a legged robot should have more than four legs for static locomotion since static walking needs, at minimum, three supporting legs to form a supporting polygon and one swing leg for a gait. A large number of legs enhance stability by making the area of the supporting polygon larger. On the other hand, an increase in the number of legs claims complex mechanisms and control. We choose a minimum number of legs for static walking.

A tetrapod, by nature, walks or runs with several gaits. A creep gait is a well-known static gait and is allowed to lift only one leg in any case⁽⁸⁾. We will implement the creep gait with our robot.

The first requirement, not to tumble over in gait, will be satisfied by the above guideline.

2.3 Grippers at the end of the legs

As shown in Figure1, the end link of each leg has a gantry-shaped mechanism. A pair of vertical links stands on the spiral in parallel. The distance between them is adjustable. A gripper is mounted on the lower end of every vertical link. Each gripper requires special mechanisms to grip the rounded rim of the spiral stably so as not to slide down in the stance phase. This gripping property fulfills the second requirement, not to slip off the spirals.

Once the gripper holds the spiral, the leg needs to maintain its foot position even if the robot body moves toward a different posture.

2.4 Positioning property of the grippers

Each gripper at the end of a leg must be placed precisely upon the rounded rim of the spiral. Otherwise, it must lose its footing since the periphery of the spirals provides discrete footholds to the walking robot. Therefore, to fulfill the third requirement, each gripper needs to be controlled to a specific position respectively. The leg mechanism should have enough DOF to control it.

2.5 Balancing of the body platform

The spiral is essentially easy to roll over on the plane ground due to its own cylindrical shape. If the robot and the spirals are tightly united and move together, it is possible that they might roll over on the steep slope of the ground due to a center-of-gravity imbalance. To maintain its balance, the body of the robot needs to be able to move freely in the horizontal plane even though the positions of the grippers continue to hold the same places on the spirals. The balancing property would fulfill the fourth requirement, not to roll over together with a gripping spiral.

2.6 Required DOF of the robot and the legs

The robot needs to have enough DOF in its own mechanism in order to move in the desired direction. Generally, 6 DOF is required for a mechanism to control arbitrary position and posture in 3-dimensional space. If we limit working space of the leg from 3-dimensional space to a 2-dimensional plane, we can reduce the DOF of each leg mechanism to three. Further we can suppress the vehicle motion of the robot. Well-coordinated motion of the four legs would produce locomotive motion toward the desired motion of the robot body.

2.7 Fulfillment of the requirements

The robot shown in Figure 1 possesses four legs. A gantry-shaped mechanism is mounted upon each leg, each of which is designated by Link13, Link14, and Link15. The gripper does not appear in Figure 1, but it will be attached at the lower end of the gantry-shaped mechanism. In the creep gait, a pair of vertical links in the gantry-shaped portion, Link 14 and Link15, takes the opening motion in the swing phase and the closing motion in the stance phase, as shown in Figure 2. In the stance phase, the grippers must hold the spiral tightly. Throughout the gait, only one leg takes the swing phase to achieve static walking.

Each leg has two prismatic joints orthogonal to each other and one rotational joint for 3 DOF motion in a plane. The prismatic joints translate Link11 in a front-back direction and Link12 in a right-left direction. The rotational joint turns Link13. Therefore, the position and posture angle of Link13 can be decided arbitrarily in the plane parallel to the body platform. We

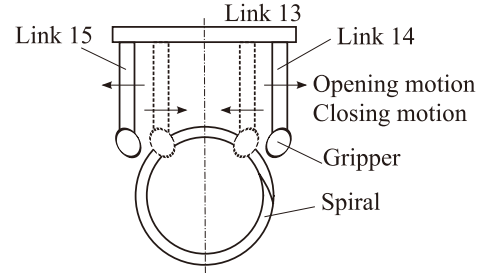


Figure 2 Leg motion to support the spiral

call this plane Link13's working space. In the gantry-shaped mechanism, there is one additional DOF of the opening/closing motion of Link14 and Link15. The working space of the grippers mounted on Link14 and Link15 forms the plane parallel to the body platform as well. When a position of the spiral and the working space of the grippers are given, a pair of the points to be gripped is derived from their intersections. By aligning Link13 to the projection of the line segment joining a pair of the points on the Link13 working space, each the gripper does not lose its footing on the spiral. In total, the leg mechanism should have enough DOF for the gripper to control to a specific position.

Since the four legs provide the same property, the position and posture angle of the robot's body can be decided within the plane parallel to the grippers' working space independently of any gripper's position. In total, the robot has enough DOF for its body to move in the desired direction.

As stated above, we can show that the conceptual design of the four-legged robot satisfies the five requirements in the previous section.

2.8 Coordinate systems

For the sake of mathematical consideration, we need to define a coordinate system at each link of the robot. Figure 3 shows the coordinate systems of the robot. The body is mounted on four legs. We denote a left front leg, a left rear leg, a right front leg, and a right rear leg as Leg1, Leg2, Leg3, and Leg4, respectively. Here we explain the coordinate systems of Leg1 as a representative of the other legs, since each leg has the same structure.

Leg1 consists of Links 11 to 15 and Grippers 14 to 15. Links 11 and 12 translate along the y_l and x_l direction by their respective prismatic joints. Link13 rotates around the center axis of Link12. Links 14 and 15 slide along Link13 symmetrically. Grippers 14 and 15 are attached at the lower end of Links 14 and 15, respectively.

The coordinate systems are set to the body and each link. The center of mass for each link is supposed to be at the link's center position. We define the origin of each coordinate system at the center of mass of the link. The x , y , and z axes are defined according to the right-handed coordinate system, as shown in Figure 3.

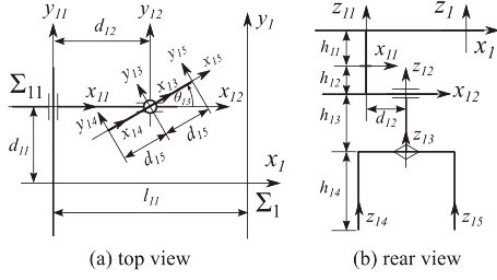


Figure 3 Coordinate systems of the robot

We denote the coordinate system of the body as Σ_1 . We denote each coordinate system of Link(ab) as $\Sigma_{(ab)}$ respectively.

2.9 Height for reducing the plant resistance

Our previous studies suggest that the resistance force against a dense stand of tall plants with hard stems is so large that a short robot does not move forward⁽⁹⁾. According to the result of an on-site experiment, when an L-shaped tapered angle of 0.1 m in width and 0.05 m in height went through the plants at 0.25 m, 0.5m, and 1 m in ground height, it received about 18 N, 3 N, and 0 N of maximum resistance force, respectively. Therefore, the robot body needs to be kept at a height greater than 1 m. We determined the diameter of the spiral at 1 m.

According to the result of another experiment, when a horizontal bar of 1 m in width went through the plants at 1 m, 1.25m, and 1.5 m in ground height, it received about 18 N, 9 N, and 7 N of maximum resistance force, respectively. Therefore we decided that the robot must maintain its body at 1.5 m in ground height to avoid resistance from a dense stand of tall plants with hard stems. Also, each leg needs to be long and thin and in an upright position.

2.10 Step motion to the next footing on the spiral

A pair of spirals on one side alternately supports the robot as footholds during its gait motion. An unresponsive spiral rotates and moves in the direction of travel for a subsequent foothold. Since the rotation mechanism has been discussed in the previous work⁽¹⁰⁾, it does not appear in Figure 1. Because of the use of

prismatic joints, the grippers slide parallel to the body platform; that is, the x_I - y_I plane, which makes the pointing motion of the gripper easier.

Typical walking robots have a mechanism to lift a foot in a swing phase, which corresponds to the gripper in our case. However as shown in Figure 2, a gantry-shaped mechanism can realize the swing phase through the opening motion instead of the lift motion. In addition, when elevation of the spiral changes from its nominal value, the vertical position of gripping the spiral can be adjusted by the distance between Link14 and Link15. The distance is narrower for higher positions, wider for lower positions.

Figure 4 shows a step motion procedure. The gantry-shaped mechanism moves from the present spiral, Sa, to the next spiral, Sb. In Figure 4(a), the end links stand on Sa. In Figure 4(b), Link14 and Link15 open and leave Sa. The balance of the robot is maintained by the other three legs. In Figure 4(c), next positions to place graspers are searched by proximity sensors that detect the spiral. In Figure 4(d), Link14 and Link15 close and the grippers hold the spiral tightly.

3 RESULTS

We defined the coordinate systems of each link in Coordinate systems. This section is devoted to deriving the kinematics and statics of the robot.

3.1 Forward kinematics

Forward kinematics of the robot is usually represented by homogeneous transformation. The 3×3 block matrix, which consists of the first 3 rows and the first 3 columns of a homogeneous transform matrix, represents a rotation matrix. The 3×1 vector, which consists of the first 3 rows in the fourth column of a homogeneous transform matrix, represents a position vector. The position vector can be used to calculate the working space of a link.

With reference to Figure 3, the homogeneous transform matrices between adjoining coordinate systems for Leg1 are as follows.

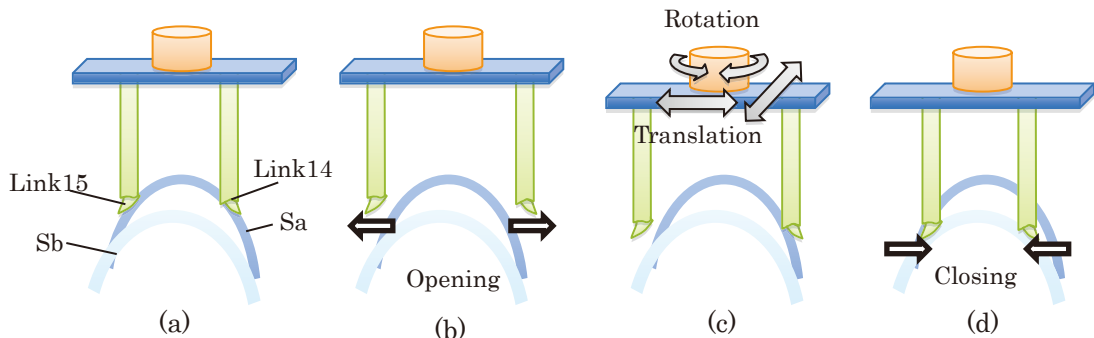


Figure 4 Procedure of a step motion to the next footing

$${}^1\mathbf{H}_{11} = \begin{bmatrix} 1 & 0 & 0 & -l_{11} \\ 0 & 1 & 0 & d_{11} \\ 0 & 0 & 1 & -h_{11} \\ 0 & 0 & 0 & 1 \end{bmatrix} \quad (1)$$

$${}^{11}\mathbf{H}_{12} = \begin{bmatrix} 1 & 0 & 0 & d_{12} \\ 0 & 1 & 0 & 0 \\ 0 & 0 & 1 & -h_{12} \\ 0 & 0 & 0 & 1 \end{bmatrix} \quad (2)$$

$${}^{12}\mathbf{H}_{13} = \begin{bmatrix} \cos\theta_{13} & -\sin\theta_{13} & 0 & 0 \\ \sin\theta_{13} & \cos\theta_{13} & 0 & 0 \\ 0 & 0 & 1 & -h_{13} \\ 0 & 0 & 0 & 1 \end{bmatrix} \quad (3)$$

$${}^{13}\mathbf{H}_{14} = \begin{bmatrix} 1 & 0 & 0 & -d_{15} \\ 0 & 1 & 0 & 0 \\ 0 & 0 & 1 & -h_{14} \\ 0 & 0 & 0 & 1 \end{bmatrix} \quad (4)$$

$${}^{13}\mathbf{H}_{15} = \begin{bmatrix} 1 & 0 & 0 & d_{15} \\ 0 & 1 & 0 & 0 \\ 0 & 0 & 1 & -h_{14} \\ 0 & 0 & 0 & 1 \end{bmatrix} \quad (5)$$

where ${}^{(a)}\mathbf{H}_{(b)}$ represents a homogeneous transform matrix from coordinate system $\langle a \rangle$ to coordinate system $\langle b \rangle$. The values of h_{11} , h_{12} , h_{13} , and h_{14} are the offset distances in the z_1 axis direction between the y_1 axis, y_{11} axis, y_{12} axis, y_{13} axis, and y_{14} axis, respectively. The value of l_{11} is the offset distance in the x_1 axis direction between y_1 axis and y_{11} axis. The variables of d_{11} , d_{12} , and d_{15} are the joint displacements in the direction of the y_1 axis, x_{11} axis, and x_{13} axis, respectively. The variable of θ_{13} is the joint angle around the z_{13} axis. The position vectors of grippers ${}^{14}\mathbf{p}_{14}$ and ${}^{15}\mathbf{p}_{15}$, with respect to Σ_{14} and Σ_{15} , are represented as follows, respectively.

$${}^{14}\mathbf{p}_{14} = \begin{bmatrix} 0 \\ 0 \\ -h_{14} \end{bmatrix} \quad {}^{15}\mathbf{p}_{15} = \begin{bmatrix} 0 \\ 0 \\ -h_{14} \end{bmatrix} \quad (6)$$

For the calculation of the working space of Link13, ${}^1\mathbf{H}_{13}$ is obtained by multiplying the successive homogeneous transform matrices.

$$\begin{aligned} {}^1\mathbf{H}_{13} &= {}^1\mathbf{H}_{11} {}^{11}\mathbf{H}_{12} {}^{12}\mathbf{H}_{13} \\ &= \begin{bmatrix} \cos\theta_{13} & -\sin\theta_{13} & 0 & -l_{11} + d_{12} \\ \sin\theta_{13} & \cos\theta_{13} & 0 & d_{11} \\ 0 & 0 & 1 & -h_{11} - h_{12} - h_{13} \\ 0 & 0 & 0 & 1 \end{bmatrix} \end{aligned} \quad (7)$$

The position vector of the origin of Σ_{13} , ${}^1\mathbf{p}_{13}$, is represented as follows.

$${}^1\mathbf{p}_{13} = \begin{bmatrix} -l_{11} + d_{12} \\ d_{11} \\ -h_{11} - h_{12} - h_{13} \end{bmatrix} \quad (8)$$

Similarly, for the calculation of the working space of grippers, ${}^1\mathbf{H}_{14}$ and ${}^1\mathbf{H}_{15}$ are obtained as follows.

$$\begin{aligned} {}^1\mathbf{H}_{14} &= {}^1\mathbf{H}_{13} {}^{13}\mathbf{H}_{14} \\ &= \begin{bmatrix} \cos\theta_{13} & -\sin\theta_{13} & 0 & -l_{11} + d_{12} - d_{15} \cos\theta_{13} \\ \sin\theta_{13} & \cos\theta_{13} & 0 & d_{11} - d_{15} \sin\theta_{13} \\ 0 & 0 & 1 & -h_{11} - h_{12} - h_{13} - h_{14} \\ 0 & 0 & 0 & 1 \end{bmatrix} \end{aligned} \quad (9)$$

$$\begin{aligned} {}^1\mathbf{H}_{15} &= {}^1\mathbf{H}_{13} {}^{13}\mathbf{H}_{15} \\ &= \begin{bmatrix} \cos\theta_{13} & -\sin\theta_{13} & 0 & -l_{11} + d_{12} + d_{15} \cos\theta_{13} \\ \sin\theta_{13} & \cos\theta_{13} & 0 & d_{11} + d_{15} \sin\theta_{13} \\ 0 & 0 & 1 & -h_{11} - h_{12} - h_{13} - h_{14} \\ 0 & 0 & 0 & 1 \end{bmatrix} \end{aligned} \quad (10)$$

The position vectors of grippers, ${}^1\mathbf{p}_{14}$ and ${}^1\mathbf{p}_{15}$, with respect to Σ_1 , are represented as follows.

$${}^1\mathbf{p}_{14} = \begin{bmatrix} -l_{11} + d_{12} - d_{15} \cos\theta_{13} \\ d_{11} - d_{15} \sin\theta_{13} \\ -h_{11} - h_{12} - h_{13} - 2h_{14} \end{bmatrix} \quad (11)$$

$${}^1\mathbf{p}_{15} = \begin{bmatrix} -l_{11} + d_{12} + d_{15} \cos\theta_{13} \\ d_{11} + d_{15} \sin\theta_{13} \\ -h_{11} - h_{12} - h_{13} - 2h_{14} \end{bmatrix} \quad (12)$$

3.2 Jacobi matrix

The Jacobi matrix is used for statics analysis or singular configuration analysis. The Jacobi matrix, \mathbf{J} , represents the relationship between the joint velocity, $\dot{\mathbf{q}}$, and the velocity of the end-point \mathbf{v} ; i.e., $\mathbf{v} = \mathbf{J}(\mathbf{q})\dot{\mathbf{q}}$. For example, in the case of Grippers 14 and 15, joint variable \mathbf{q} would be $\mathbf{q} = [d_{11} \ d_{12} \ \theta_{13} \ d_{15}]^T$, and the velocity of each gripper would be $\mathbf{v} = [v_x \ v_y \ \omega_z]^T$, where v_x and v_y are the components of the gripper velocity in the direction of x_1 and y_1 axes, respectively, and ω_z represents the components of the gripper rotational velocity in the direction of z_1 axis. The Jacobi matrix of Gripper 14, \mathbf{J}_{14} , is obtained by calculating the partial differentiation of ${}^1\mathbf{p}_{14}$ and the corresponding rotating vectors.

$$\mathbf{J}_{14} = \begin{bmatrix} 0 & 1 & d_{15} \sin\theta_{13} & -\cos\theta_{13} \\ 1 & 0 & -d_{15} \cos\theta_{13} & -\sin\theta_{13} \\ 0 & 0 & 1 & 0 \end{bmatrix} \quad (13)$$

Similarly, the Jacobi matrix of Gripper 15, \mathbf{J}_{15} , is obtained as follows.

$$J_{15} = \begin{bmatrix} 0 & 1 & -d_{15} \sin \theta_{13} & \cos \theta_{13} \\ 1 & 0 & d_{15} \cos \theta_{13} & \sin \theta_{13} \\ 0 & 0 & 1 & 0 \end{bmatrix} \quad (14)$$

The Jacobi matrix of Link 13, J_{13} , is much simpler.

$$J_{13} = \begin{bmatrix} 0 & 1 & 0 & 0 \\ 1 & 0 & 0 & 0 \\ 0 & 0 & 1 & 0 \end{bmatrix} \quad (15)$$

3.3 Inverse kinematics

Once the gripper positions are given, the joint parameters can be obtained through inverse kinematics. Suppose that ${}^1\mathbf{p}_{14} = [x_{14} \ y_{14} \ z_{14}]^T$ and ${}^1\mathbf{p}_{15} = [x_{15} \ y_{15} \ z_{15}]^T$. The following formulas can be derived from Eqs. (11)-(12):

$$d_{15} = \frac{\sqrt{(x_{15}-x_{14})^2+(y_{15}-y_{14})^2}}{2} \quad (16)$$

$$\theta_{13} = \tan^{-1} \frac{y_{15}-y_{14}}{x_{15}-x_{14}} \quad (17)$$

$$d_{12} = l_{11} + x_{15} - d_{15} \cos \theta_{13} \quad (18)$$

$$d_{11} = y_{15} + d_{15} \sin \theta_{13} \quad (19)$$

These formulas provide the joint parameters for Leg1. The other joint parameters can be obtained in a similar manner.

3.4 Statics

Using a transposition of the Jacobi matrix, the following relationship is derived.

$$\boldsymbol{\tau} = J(\mathbf{q})^T \mathbf{f} \quad (20)$$

Where $\boldsymbol{\tau}$ is a force/torque vector in the joint space and \mathbf{f} is a force/torque vector in the working space. Suppose that force/torque vectors at Grippers 14 and 15 are denoted as \mathbf{f}_{14} and \mathbf{f}_{15} , respectively. The resultant force/torque vectors in the joint space, $\boldsymbol{\tau}_{14}$ and $\boldsymbol{\tau}_{15}$, from \mathbf{f}_{14} and \mathbf{f}_{15} are respectively obtained as follows.

$$\boldsymbol{\tau}_{14} = \begin{bmatrix} 0 & 1 & 0 \\ 1 & 0 & 0 \\ d_{15} \sin \theta_{13} & -d_{15} \cos \theta_{13} & 1 \\ -\cos \theta_{13} & -\sin \theta_{13} & 0 \end{bmatrix} \mathbf{f}_{14} \quad (21)$$

$$\boldsymbol{\tau}_{15} = \begin{bmatrix} 0 & 1 & 0 \\ 1 & 0 & 0 \\ -d_{15} \sin \theta_{13} & d_{15} \cos \theta_{13} & 1 \\ \cos \theta_{13} & \sin \theta_{13} & 0 \end{bmatrix} \mathbf{f}_{15} \quad (22)$$

The statics formulas, other than Leg1, can be obtained in a similar manner.

4 DISCUSSION

We qualitatively demonstrated the conceptual design of the robot and its validity. In this section, we confirm the validity through the formulas derived in kinematic and statics section.

First of all, the positioning property of the grippers is easy to confirm through the inverse kinematics. We can calculate the joint parameters for any gripper positions of $[x_{14} \ y_{14}]^T$ and $[x_{15} \ y_{15}]^T$ using Eqs.(16), (17), (18), and (19).

Secondly, the body movement property for the balancing capability of the body platform is verified. Since all grippers' positions are fixed, d_{15} is a constant and $\dot{d}_{15} = 0$. Therefore, each gantry-shaped mechanism is regarded as one link and as a part of the spiral that is gripped by the mechanism. It is enough to consider the movement of Link13 instead of the grippers for Leg1. Multiplying J_{13} by the velocity vector $[\dot{d}_{11} \ \dot{d}_{12} \ \dot{\theta}_{13} \ 0]^T$, we get

$$\begin{bmatrix} 0 & 1 & 0 & 0 \\ 1 & 0 & 0 & 0 \\ 0 & 0 & 1 & 0 \end{bmatrix} \begin{bmatrix} \dot{d}_{11} \\ \dot{d}_{12} \\ \dot{\theta}_{13} \\ 0 \end{bmatrix} = \begin{bmatrix} \dot{d}_{12} \\ \dot{d}_{11} \\ \dot{\theta}_{13} \end{bmatrix}. \quad (23)$$

This equation shows that, for Leg1, \mathbf{v} at the origin of Σ_{13} is decided by \dot{d}_{11} , \dot{d}_{12} , and $\dot{\theta}_{13}$ independently. The other legs supporting the body platform have the same properties. Hence, the body velocity can be arbitrarily decided by adjusting the joint velocities even if all the grippers' positions are fixed.

In addition, the 3×3 block matrix consisting of the first 3 columns of J_{13} is a nonsingular matrix. It means that the robot has no singular configuration. This is a desirable property in controlling the robot.

Thirdly, it is verified that the robot has enough DOF in its own mechanism in order to move in the desired direction. In advance, we investigate whether the working space of Link13 or grippers is a plane parallel to the x_1y_1 plane in Σ_1 . The normal vector of the x_1y_1 plane can be denoted as $\mathbf{n} = [0 \ 0 \ 1]^T$. Suppose that there are two different pairs of values for the joint parameter (d_{11}, d_{12}) , $(\bar{d}_{11}, \bar{d}_{12})$ and $(\widetilde{d}_{11}, \widetilde{d}_{12})$, and the corresponding position vectors ${}^1\mathbf{p}_{13}$ and ${}^1\widetilde{\mathbf{p}}_{13}$ using Eq. (8), respectively. Then, the following equation is satisfied.

$$\begin{aligned} & \mathbf{n}^T (\overline{{}^1\mathbf{p}_{13}} - \widetilde{{}^1\mathbf{p}_{13}}) \\ &= [0 \quad 0 \quad 1] \begin{bmatrix} \overline{d_{12}} - \widetilde{d_{12}} \\ \overline{d_{11}} - \widetilde{d_{11}} \\ 0 \end{bmatrix} = 0. \end{aligned} \quad () \quad 24$$

Therefore, it is proved that the space formed by ${}^1\mathbf{p}_{13}$ is parallel to the x_1y_1 plane. In the same way, the space formed by ${}^1\mathbf{p}_{14}$ or ${}^1\mathbf{p}_{15}$ is parallel to the x_1y_1 plane. As mentioned above, in the working space of Link13, the body velocity can be arbitrarily decided by adjusting the joint velocities. Therefore, we can conclude that the robot has enough DOF.

In addition, since the working space is parallel to the x_1y_1 plane, it is understood that there is no vertical motion.

Finally we deduce one characteristic property about the statics. Assuming that \mathbf{f}_{14} is equal to \mathbf{f}_{15} and adding $\boldsymbol{\tau}_{15}$ to $\boldsymbol{\tau}_{14}$, we get

$$\frac{\boldsymbol{\tau}_{14} + \boldsymbol{\tau}_{15}}{2} = \begin{bmatrix} 0 & 1 & 0 \\ 1 & 0 & 0 \\ 0 & 0 & 1 \\ 0 & 0 & 0 \end{bmatrix} \mathbf{f}_{14} = \mathbf{J}_{13}^T \mathbf{f}_{14}. \quad (25)$$

If the external forces/torques \mathbf{f}_{14} and \mathbf{f}_{15} are exerted on a pair of the graspers in phase, its components are independently related to the forces/torques of Joint 11, 12, and 13, respectively. Subtracting $\boldsymbol{\tau}_{15}$ from $\boldsymbol{\tau}_{14}$, we get

$$\begin{aligned} & \frac{\boldsymbol{\tau}_{14} - \boldsymbol{\tau}_{15}}{2} \\ &= \begin{bmatrix} 0 & 0 & 0 \\ 0 & 0 & 0 \\ d_{15} \sin \theta_{13} & -d_{15} \cos \theta_{13} & 0 \\ -\cos \theta_{13} & -\sin \theta_{13} & 0 \end{bmatrix} \mathbf{f}_{14}. \end{aligned} \quad () \quad 26$$

If the external forces/torques \mathbf{f}_{14} and \mathbf{f}_{15} are exerted on a pair of the graspers in anti-phase, the resultant forces of Link11 and Link12 became zero. In particular, the torque does not transmit to any joint.

5 CONCLUSION

We described the new conceptual design of a four-legged robot for a double-spiral mobile architecture. The robot consists of two pairs of spirals and one mobile robot. Based on the requirement for the secure walking motion, the concept of design was explained. Kinematics and statics of the robot were derived, and then the validity of the design was explained using the formulas.

The main contribution of the new design is the use of a gantry-shaped mechanism for legs and the realization of a swing phase without any vertical motion. Employing a pair of prismatic joints orthogonal to each other limits the working space of the leg to a horizontal plane. These suppress vertical motion and enhance the walking security. The assembly of the robot and the experiment are left for future work

ACKNOWLEDGMENT

This work was supported by JSPS KAKENHI Grant Number 24560282. The authors also express their heartfelt thanks to Center of Environmental Science and Disaster Mitigation for Advanced Research (CEDAR) of Muroran Institute of Technology for meaningful assistance.

REFERENCES

- (1) Kondo, N., Noguchi, S., and Kadota, M., Agriculture robots (in Japanese), Corona publishing, (2004).
- (2) Thorpe, C. E., Vision and Navigation, The Carnegie Mellon Navlab, Kluwer Academic, (1990).
- (3) Tadokoro, S., Rescue Robotics: DDT Project on Robots and Systems for Urban Search and Rescue, Springer, (2010).
- (4) Cole, B. N., Inquiry into amphibious screw traction, Proceedings of the Institution of Mechanical Engineers 1847–1982, 175(19), (1961), 919–940.
- (5) Neumeyer, M. and Jones, B., The marsh screw amphibian, Journal of Terramechanics, 2(4), (1965), p83–88.
- (6) Nagaoka, K., Otsuki, M. and Kubota, T., Study on screw rover specialized for locomotion on lunar soil, Proceedings of the 2009 Japan Society of Mechanical Engineers Conference on Robotics and Mechatronics, (in Japanese), (2009), 1A2-F17(1)–1A2-F17(4).
- (7) Hanajima, N., Hayasaka, Y., Azumi, N., Kawauchi, K., Yamashita, M. and Hikita, H., Double Spiral propulsion mechanism in wetlands, Joint Seminar on Environmental Science and Disaster Mitigation Research 2009, (2009), p77-78.
- (8) McGhee, R. B. and Frank, A. A., On the Stability Properties of Quadruped Creeping Gaits, Mathematical Biosciences, 3, (1968), 331-351.
- (9) Hayasaka, Y., Hanajima, N., Kawauchi, K., Yamashita, M. and Hikita, H., Development of a spiral propulsion mechanism for locomotion on wetlands (Locomotion characteristic and drive mechanism), In proceedings of 14th Robotics Symposia, (2009), p282-287.
- (10) Liu, Q., Hanajima, N., Kawauchi, K., Yamashita, M., Hikita, H. and Kazama, T., Kinematic Modeling and Analysis of a Serial-Parallel Field Robot with Variable Structure, Chiang-Mai University Journal of Natural Sciences - Special Issue on Manufacturing Technology, 10(1), (2011), p127-139.